The ^{181}Ta Nuclear Quadrupole Interaction in the Charge Density Wave Phases of 1 T-TaS_2 *

P. Ganal[a], T. Butz[a], A. Lerf[b], M. Naito[c], and H. Nishihara[d]

[a] Physik-Department, Technische Universität München, Garching, FRG
[b] Walther-Meißner-Institut für Tieftemperaturforschung der Bayerischen Akademie der Wissenschaften, Garching, FRG
[c] NTT Basic Research Laboratories, 3-9-11 Midoricho, Musashino-shi, Tokyo 180, Japan.
[d] Faculty of Science and Technology, Ryukoku University, Seta-ooecho 1, Ohtsu 520-21, Japan.

Z. Naturforsch. **45a**, 439–444 (1990); received August 22, 1989

With a high resolution time differential perturbed angular correlation spectrometer we investigated the nuclear quadrupole interaction of ^{181}Ta in 1 T-TaS_2. The results obtained for the commensurate charge density wave phase lead to a revised assignment of the previously observed ^{181}Ta NQR resonances. Differences in the intra-cluster architecture of the 13-atom Star of David cluster between 1 T-TaS_2 and 1 T-$TaSe_2$ could be responsible for the metal to semiconductor transition which occurs in 1 T-TaS_2 but not in 1 T-$TaSe_2$.

1. Introduction

The layered compounds 1 T-TaS_2 and 1 T-$TaSe_2$ exhibit a commensurate $\sqrt{13}a_0 \times \sqrt{13}a_0$ superstructure at low temperatures which is commonly described in terms of the formation of a charge density wave/periodic lattice distortion (CDW/PLD). This $3\boldsymbol{q}$-superstructure leads to a charge density pattern shown in Fig. 1 a and a corresponding lattice distortion as shown in Fig. 1 b. The undistorted Star of David 13-atom cluster consists of three inequivalent Ta atoms with populations $\alpha:\beta:\gamma = 1:6:6$. The central site α has axial symmetry whereas the symmetry at the peripheral β- and γ-sites is broken. Previous attempts to observe these inequivalent Ta sites via the ^{181}Ta nuclear quadrupole interaction by Mössbauer spectroscopy (ME) and time differential perturbed angular correlations (TDPAC) were partly successful only: only the two prominent sites were detected by ME in 1 T-$TaSe_2$ [1]; no ME resonances were observed in 1 T-TaS_2; by TDPAC only the two prominent sites were detected in 1 T-TaS_2 [2]. Recent NMR and NQR studies of powder and single crystal samples of both 1 T-TaS_2 [3] and 1 T-$TaSe_2$ [4] were much more successful: a total of seven inequivalent Ta sites, denoted by α, β_{1-3}, γ_{1-3}, for 1 T-$TaSe_2$ and a total of thirteen inequivalent Ta sites, denoted by α, β_{1-6}, γ_{1-6}, for 1 T-TaS_2 were observed, which show that the Star of David clusters are further distorted. However, there was a severe discrepancy in the derived hyperfine parameters between the NMR/NQR data and the TDPAC data for 1 T-TaS_2 [2]. We therefore repeated the TDPAC measurements with a new spectrometer equipped with BaF_2-scintillators with a very good time resolution. This allowed the observation of *all* precession frequencies up to about 3 Grad/s. Thus, there is no ambiguity in the assignment of the observed frequencies, contrary to the set of NQR data, which did *not* contain *all* resonances. Although the frequency resolution of ^{181}Ta TDPAC is very poor compared to ^{181}Ta NQR, it has the advantage that site populations can be reliably deduced. Both techniques combined lead to a reassignment of the NQR frequencies and now yield a very detailed picture of the intra-cluster architecture. There are marked differences between the cluster in 1 T-TaS_2 and 1 T-$TaSe_2$ – which were not apparent previously due to the erroneous assignment – both as far as the distortion and the charge distribution are concerned.

2. Experimental

The TDPAC experiments were performed on the 133 keV–482 keV γ-γ-cascade in ^{181}Ta which is produced via β-decay from ^{181}Hf. Therefore we doped our 1 T-TaS_2 samples with approximately 200 ppm

* Presented at the Xth International Symbosium on Nuclear Quadrupole Resonance Spectroscopy, Takayama, Japan, August 22–26, 1989.

Reprint requests to Dr. T. Butz, Physik-Department E 15, Technische Universität München, D-8046 Garching.

0932-0784 / 90 / 0300-0439 $ 01.30/0. – Please order a reprint rather than making your own copy.

Dieses Werk wurde im Jahr 2013 vom Verlag Zeitschrift für Naturforschung in Zusammenarbeit mit der Max-Planck-Gesellschaft zur Förderung der Wissenschaften e.V. digitalisiert und unter folgender Lizenz veröffentlicht: Creative Commons Namensnennung-Keine Bearbeitung 3.0 Deutschland Lizenz.

This work has been digitalized and published in 2013 by Verlag Zeitschrift für Naturforschung in cooperation with the Max Planck Society for the Advancement of Science under a Creative Commons Attribution-NoDerivs 3.0 Germany License.

Zum 01.01.2015 ist eine Anpassung der Lizenzbedingungen (Entfall der Creative Commons Lizenzbedingung „Keine Bearbeitung") beabsichtigt, um eine Nachnutzung auch im Rahmen zukünftiger wissenschaftlicher Nutzungsformen zu ermöglichen.

On 01.01.2015 it is planned to change the License Conditions (the removal of the Creative Commons License condition "no derivative works"). This is to allow reuse in the area of future scientific usage.

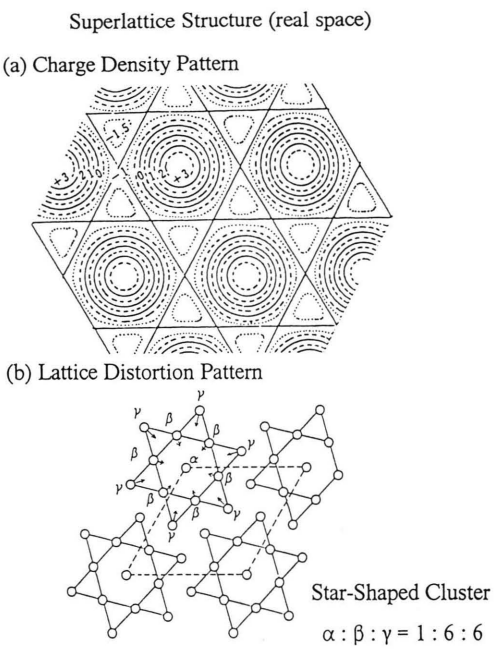

Fig. 1. The commensurate $\sqrt{13}a_0 \times \sqrt{13}a_0$ CDW phase: a) charge density pattern, b) lattice distortion pattern.

neutron activated Hf metal during iodine vapour transport crystal growth. The start level of the γ-γ-cascade is sufficiently long-lived ($t_{1/2} = 17$ μs) to allow for electronic re-arrangements after the β-decay before the actual measurement on the γ-γ-cascade starts. This is particularly important in the case of CDW's: the CDW is very likely to be pinned at the impurity Hf [5]; after nuclear transmutation to Ta – which is now a constituent of the lattice – the CDW can re-arrange.

We used a conventional 4-detector fast-slow coincidence setup. However, we now used conical BaF_2-scintillators with a time resolution of about 450 ps for the 133 keV–482 keV cascade. The detectors were arranged at 90° intervals in a plane. Eight out of twelve possible coincidence subgroups were stored simultaneously and combined in the following way:

$$A_2 G_2 = 2 \frac{\sqrt[4]{W_{13} W_{31} W_{24} W_{42}} - \sqrt[4]{W_{14} W_{41} W_{23} W_{32}}}{\sqrt[4]{W_{13} W_{31} W_{24} W_{42}} + 2\sqrt[4]{W_{14} W_{41} W_{23} W_{32}}}, \quad (1)$$

where W_{ij} denotes the coincidence countrate between detector i (133 keV) and detector j (482 keV), already corrected for chance coincidences.

We performed measurements with a stack of single crystals oriented along the c-axis but random along the a-axis/b-axis.

Three different geometries were employed:

1Ω: V_{zz} is normal to the detector plane. This yields essentially the fundamental frequency only with maximum intensity $\hbar\omega = E_{\pm 3/2} - E_{\pm 1/2}$.

2Ω: V_{zz} in the detector plane halfway between two detectors. This yields the first harmonic $\hbar\omega' = E_{\pm 5/2} - E_{\pm 3/2}$ with maximum intensity and a smaller contribution of ω.

3Ω: V_{zz} tilted 45° with respect to the detector plane and halfway between two detectors. This yields the second harmonic $\hbar\omega'' = E_{+5/2} - E_{+1/2}$ with maximum possible intensity. However, the spectra are still dominated by contributions of ω and ω'.

The 1Ω-geometry is not well suited for studies which require a good frequency resolution; however, it is ideally suited for a search for sites with a small population. The 2Ω-geometry is ideally suited for high-resolution studies and has still a high sensitivity; however, it does not lead to an ambiguous assignment of resolved first harmonic peaks to unresolved fundamental peaks. Here, the 3Ω-geometry which yields *all* precession frequencies is required; since we always have $\omega'' = \omega + \omega'$, it suffices to resolve both harmonics in order to obtain an ambiguous assignment. Its disadvantage is the poor sensitivity for ω' and ω''.

All TDPAC data were least squares fitted and Fourier transformed in order to facilitate the extraction of the number and population of inequivalent Ta sites as well as the strength and symmetry of the nuclear quadrupole interaction at these sites.

3. Results

In Fig 2 the TDPAC spectra (left) and their Fourier transforms (right) are shown for 1 T-TaS_2 at 13 K in all three different geometries. The two prominent peaks (labelled ω_1 and ω_2) with equal intensity are immediately visible, including their harmonics. Whereas ω'_1 is significantly broadened, ω'_2 is relatively sharp. This suggests that each of the six peripheral Ta atoms are actually slightly inequivalent. The detection of the center site (labelled ω_3) is much more difficult. The fundamental is buried under the fundamental of ω_1 and leads to a barely visible left shoulder of ω_1 only. Its second harmonic ω''_3 is also buried under the second harmonic of ω''_1. However, its first harmonic ω'_3 is just resolved on the high frequency side of ω'_1, most clearly visible in the 2Ω-geometry. This rather unexpected position of the center site signal explains

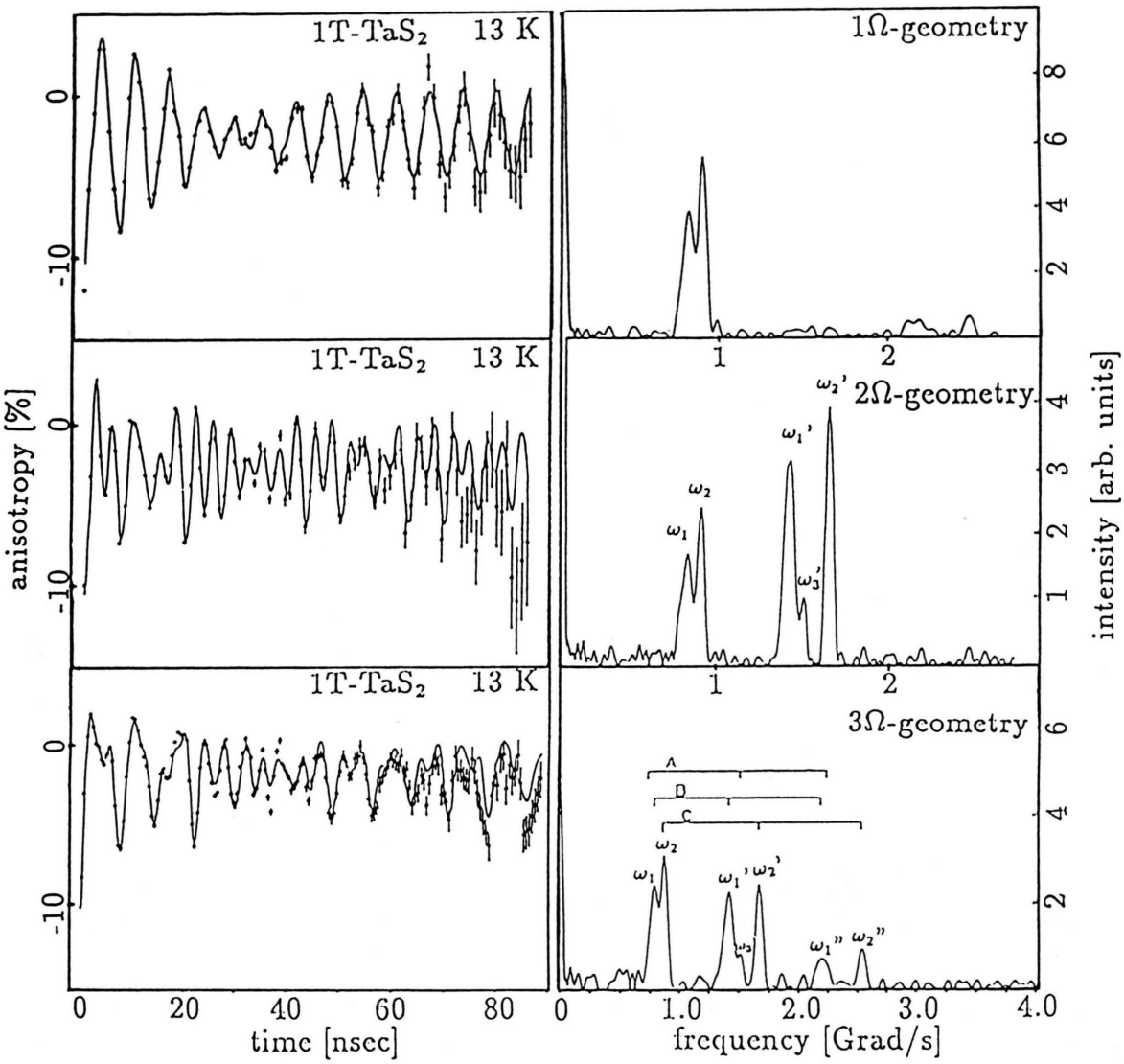

Fig. 2. TDPAC spectra (left) and their Fourier transform (right) for ^{181}Ta in 1 T-TaS_2 at 13 K for three different crystal orientations.

why previous attempts to search for this unique site with a poor time resolution failed [2].

A least squares analysis with three inequivalent sites A, B, and C and adjustable line broadening for the B- and C-sites yields the unambiguous assignment as shown in the bar-diagram in Fig. 2, bottom.

Instead of presenting further details of the least squares analysis of the TDPAC data alone we now follow a different route: the present TDPAC data are in complete disagreement with the previously derived hyperfine parameters from NQR measurements [3]; hence, we shall try to re-assign the NQR resonances and then extract the set of hyperfine parameters which best agrees with *both* the TDPAC and NQR data. This will be done in the next section.

4. Discussion

The previously observed NQR-pattern for 1 T-TaS_2 at 4.2 K is shown in Fig. 3 [3]. In that paper a different assignment of the resonances was given: the partly re-

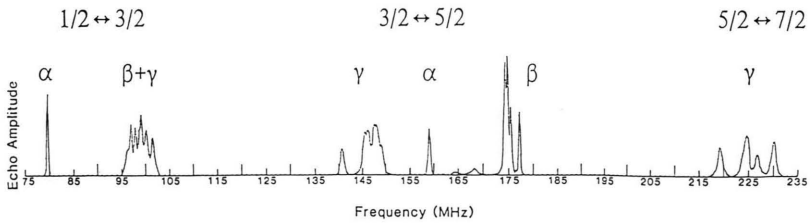

Fig. 3. NQR pattern for 1 T-TaS_2 at 4.2 K showing the revised peak assignment.

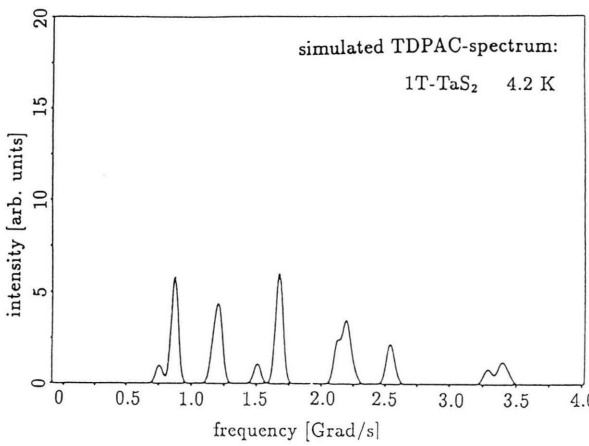

Fig. 4. Simulated TDPAC spectrum of 1 T-TaS_2 at 4.2 K, based on the hyperfine parameters derived from the earlier NQR peak assignment [3].

Table 1. Hyperfine parameters of the 13-atom star shaped cluster in 1 T-TaS_2 and 1 T-$TaSe_2$ at 4.2/13 K.

Site	1 T-TaS_2		1 T-$TaSe_2$	
	V_{zz} [10^{18} V/cm^2]	η_{NQR}	V_{zz} [10^{18} V/cm^2]	η_{NQR}
α	−1.399	0.021	−1.018	0.173
β_1	−1.579	0.161	−1.532	0.191
β_2	−1.564	0.162	−1.551	0.225
β_3	−1.558	0.183	−1.567	0.287
β_4	−1.560	0.186	–	–
β_5	−1.566	0.193	–	–
β_6	−1.568	0.203	–	–
γ_1	−1.345	0.283	−1.503	0.176
γ_2	−1.361	0.289	−1.524	0.248
γ_3	−1.329	0.298	−1.489	0.305
γ_4	−1.342	0.311	–	–
γ_5	−1.363	0.319	–	–
γ_6	−1.301	0.345	–	–

solved structure between 95 MHz and 103 MHz was entirely attributed to the β-sites alone and the peaks around 140–150 MHz were assigned to the $1/2 \leftrightarrow 3/2$ transition of the γ-sites. Consequently, the peaks around 218–232 MHz were assigned to the $3/2 \leftrightarrow 5/2$ transition of the γ-sites. A simulated TDPAC spectrum with the hyperfine parameters based on this old assignment is shown in Fig. 4 and is clearly in complete disagreement with our observed data (see Figure 2). Hence, we propose now the revised assignment as shown in Fig. 3: for the ground state of ^{181}Ta with $I = 7/2$ and the given hyperfine parameters (strength *and* asymmetry parameter η) it just happens that the β- and γ-resonances for $1/2 \leftrightarrow 3/2$ overlap; on the contrary, for the 482 keV excited state of ^{181}Ta with $I = 5/2$ the β- and γ-frequencies are well separated. It should be mentioned that all observed line intensities in the TDPAC data are consistent with V_{zz} being perpendicular to the layers. However, the intensities depend on a possible tilt angle to second order only, and hence the accuracy is limited to approximately 5–10°. In fact, the NMR data are slightly but systematically shifted from what would be expected from the NQR data as far as η is concerned. This small shift could be due to a small tilt angle of V_{zz} with respect to the plane normal.

With this revised assignment, perfect agreement between the NQR and the TDPAC data is achieved. The derived parameters for the electric field gradient V_{zz} and η_{NQR} which fit both the NQR and the TDPAC data best – including the further constraints regarding η from NMR measurements – are listed in Table 1 (here we used $Q_{5/2} = 2.36(5)$ b [6]). The inequivalent Ta sites are labelled in ascending order of η. For comparison, the data for 1 T-$TaSe_2$ are also listed [4]. Here, the assignment to β- and γ-sites is based on the observed relaxation behaviour [4]. The β-sites are assumed to be subjected to the largest V_{zz}. Note that the sign of V_{zz} is negative as derived from ME measurements [1].

There are several remarkable differences between 1 T-TaS_2 and 1 T-$TaSe_2$:

(i) In 1 T-TaS_2, the 13 atoms of the Star of David cluster are all inequivalent, whereas in 1 T-$TaSe_2$ two

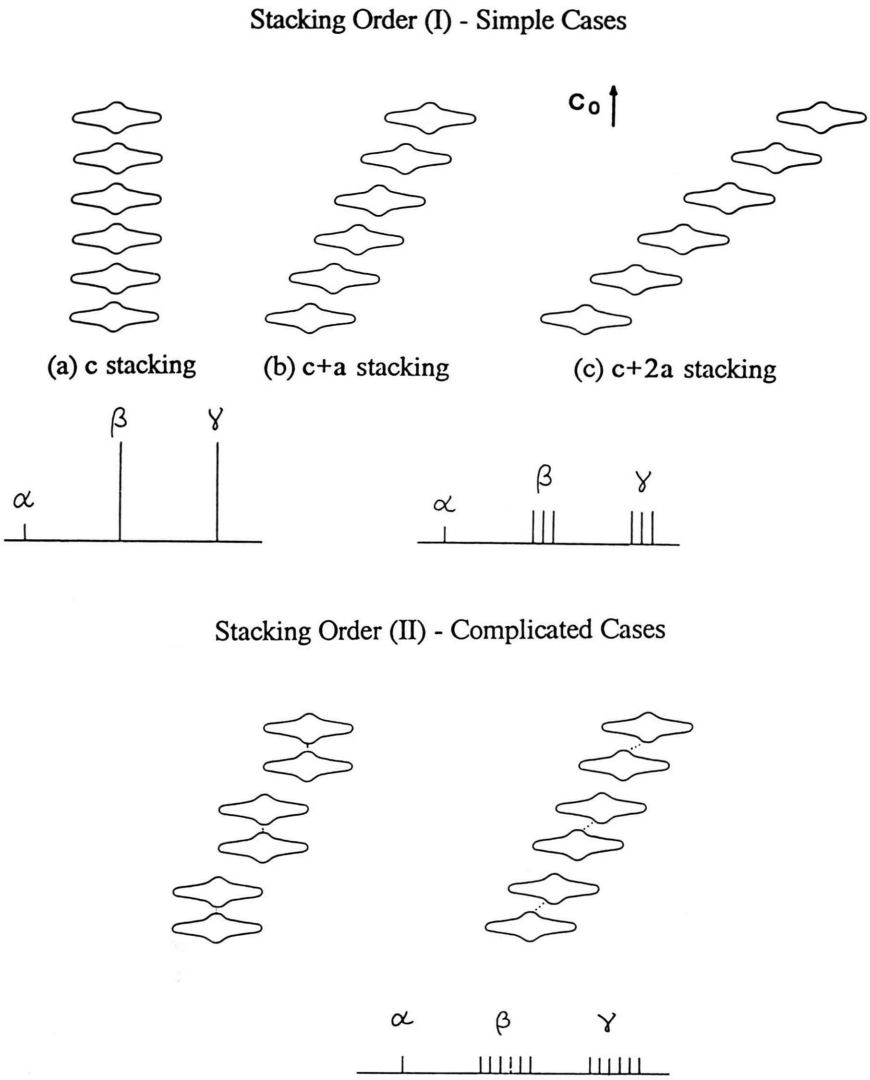

Fig. 5. Various stacking schemes for the CDW leading to an undistorted 1:6:6 pattern and to a partial and complete separation into inequivalent Ta sites.

each are equivalent. This leads to the CDW stacking scheme proposed in Figure 5. Whereas the c+2a stacking pertains to 1 T-$TaSe_2$, the stacking order of type II is proposed for 1 T-TaS_2. The undistorted Star of David with populations 1:6:6 was recently observed for 6R-TaS_2 at temperatures above about 50 K, where the CDW forms in every second sandwich only [7].

(ii) Whereas the values for V_{zz} between the β- and γ-sites of 1 T-TaS_2 differ markedly, they are almost identical for 1 T-$TaSe_2$. This was already noted previously by ME measurements on 1 T-$TaSe_2$ at 300 K [1].

(iii) The center site α does not possess axial symmetry, particularly so for 1 T-$TaSe_2$. This loss of axial symmetry is a consequence of the distortion of the Star of David cluster.

(iv) The most striking difference between 1 T-$TaSe_2$ and 1 T-TaS_2 concerns the *magnitude* of V_{zz} at the center site α: whereas it is about 30% *lower* compared to the β- and γ-sites in 1 T-$TaSe_2$, it is *intermediate* between the β- and γ-site values in 1 T-TaS_2. A reduc-

tion of the electric field gradient upon charge transfer is generally observed for intercalation compounds of 2H-TaS_2 [8] and 1T-TaS_2 [9]. Hence, the result for 1T-$TaSe_2$ is quite expected and considered "normal". On the contrary, the high value for V_{zz} in 1T-TaS_2 at the α-site suggests that although there is indeed the maximum charge density it is not in the same orbitals as far as symmetry is concerned as in 1T-$TaSe_2$.

This clearly shows that the charge distribution inside the 13-atom cluster must be very different for both systems. Such a behaviour was recently observed by scanning tunneling microscopy [10]. Although the overall shape of the cluster seems to be very similar – with all distortions being larger in 1T-$TaSe_2$ than in 1T-TaS_2 –, judging from room temperature X-ray diffraction data [11], the intra-cluster architecture must be very dissimilar. It should be pointed out that the electric field gradient results from the $l=2$ multipole component of the charge density distribution only and certainly does not simply scale like the charge density itself, as sometimes assumed.

The metal to semiconductor transition of 1T-TaS_2 and not of 1T-$TaSe_2$ is possibly related to this different intra-cluster architecture. A pairing of two clusters in neighbouring layers – note that the actual cluster consists of 13 Ta atoms and 2×13 S atoms – would lead to a pairing of the two unpaired electrons of each cluster and thus to the semiconductor transition. However, we have performed extensive measurements by TDPAC on 1T-TaS_2 in the entire temperature range from 13 K to 540 K (to be published in a forthcoming paper) which do *not* support the idea that the intra-cluster architecture changes from the "normal" 1T-$TaSe_2$ behaviour to the "abnormal" 1T-TaS_2 behaviour upon lock-in around 200 K. Therefore, two types of clusters appear to be formed in 1T-TaS_2 and 1T-$TaSe_2$ right upon the CDW onset (which, unfortunately, cannot be observed because the samples transform to the 2H-modification prior to the expected onset temperature). One type of cluster undergoes the metal to semiconductor transition while the other type remains metallic. Apparently, the interlayer coupling plays an important role in this respect.

Acknowledgements

The continuous interest and support by Profs. G. M. Kalvius and K. Andres is gratefully acknowledged. It is a pleasure to thank Dr. S. Saibene for the fruitful cooperation. This work was supported in part by the Bundesministerium für Forschung und Technologie, FRG under 03-KA1TUM.

[1] L. Pfeiffer, T. Kovacs, and F. J. DiSalvo, Hyperfine Interactions **4,** 803 (1978); Phys. Rev. Lett. **52,** 687 (1984).
[2] T. Butz, A. Vasquez, and A. Lerf, J. Phys. **C 12,** 4509 (1979).
[3] M. Naito, H. Nishihara, and S. Tanaka, J. Phys. Soc. Japan **7,** 2410 (1986).
[4] M. Naito, H. Nishihara, and S. Tanaka, J. Phys. Soc. Japan **54,** 3946 (1985).
[5] H. P. Hughes and R. A. Pollak, Phil. Mag. **34,** 1025 (1976).
[6] T. Butz and A. Lerf, Phys. Lett. **97A,** 217 (1983).
[7] S. Saibene, Ph.D. thesis, Technische Universität München, FRG, unpublished.
[8] T. Butz and A. Lerf, Rev. Chim. Miner. **19,** 296 (1982).
[9] P. Ganal, T. Butz, and A. Lerf, Synthetic Metals, in press.
[10] R. V. Coleman, B. Giambattista, P. K. Hansma, A. Johnson, W. W. McNairy, and C. G. Slough, Adv. Phys. **37,** 559 (1988).
[11] R. Brouwer and F. Jellinek, Physica **99B,** 51 (1980).